Vol. 15 (2026): Proceedings of the 2026 International Conference on Mathematics, Physics and Earth Sciences (IC-MPES 2026)
E-ISSN: 3105-0522 P-ISSN: 3105-0514
DOI: https://doi.org/10.70267/icmpes.20261588100

The Density Distribution of Dark Matter in the Milky Way Based on Stellar Velocities Measured by GAIA DR2

Yuxin Qin*

Shenzhen College of International Education, Shenzhen, China

**Corresponding author: Yuxin Qin.*

Abstract

Since the early stages of the formation of the universe, dark matter has played a crucial role in mapping the large scale structures, being the frame of matter overdensities which grew up to form galactic and intergalactic structures. However, due to its mysterious nature and the property only interacting with gravitational fields, not much light is shed on the discovery and understanding of dark matter's possible particle nature. This paper aims to interpret the density distribution of dark matter in different regions of the Milky Way(Bulge, Disk, Halo) from most recent models(NFW, Einasto, Isothermal, Burkert, Moore) and match it with the data of stellar rotational velocities measured by GAIA DR2 database. We do not directly derive velocities from raw GAIA DR2, but instead use compiled rotation curve data calibrated with GAIA measurements taken from Sofue et al. 2025[20]. We have also extrapolated parameters and normalization factors regarding each model, and evaluated with a more rudimentary method offered from Cirelli, M. et al. 2011[7]. Through our method, we provide a rudimentary overview on how the dark matter density profiles correlate with the newest DR2 data and evaluate their applicability. In turn, we hope the results offer insight on which model could be compatible concurrently in our galaxy.

Keywords

galaxies, dark matter, milky way, rotation curve, dark matter density

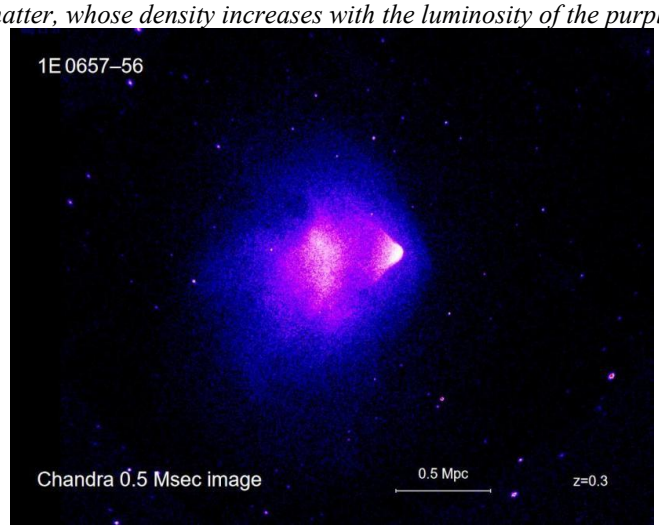
1. Modern History of Dark Matter Research

Entering the late 20th and 21st century, there has been dark matter evidence measured in galactic rotational curves, galaxy clusters (e.g. Bullet cluster shown in Fig.1) and through the Cosmic Microwave Background anisotropy data, a primordial form of light generated about 380.000 years after the Universe formation. Theories and hypotheses about the nature of dark matter are also blooming in the cosmology field, suggesting it is composed of axions, WIMPs, MACHOs, or even non-existent according to MOND, for which dark matter evidence should be explained with a modification of the Newtonian theory of gravity. There are several particle physics theories of dark matter and several of them have been strongly constrained with current experiments and observations. However, with the development of technology and instruments targeted towards discovering dark matter (e.g XENON, LUX, PandaX) and even multi-messenger paths such as LIGO, we are discovering more gravitational evidence of dark matter that raises even more questions about its origin, properties, and purpose.

By carrying on the ancient yet reliable method of tracking stellar velocities into rotational curves, we expect to improve knowledge about the dark matter distribution model of the Milky Way with the newest GAIA DR2 data.

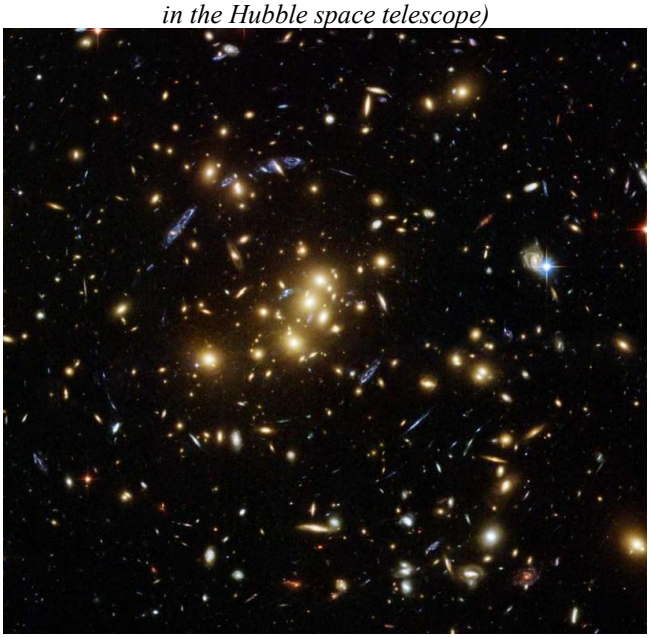
The observation of the Bullet Cluster, of which we show an image below, is one of the most interesting pieces of evidence of dark matter. This represents the collision of two Clusters of Galaxies. We see in the image in magenta the location of the hot gas that is displaced with respect to the center of the Gravitational lensing, which represents where the dark matter is distributed. This observation typically leads to the conclusion that dark matter particles should be very weakly self interacting.

Figure 1: Bullet Cluster Image in X-ray, redshift 0.3z, exposure 0.5 megaseconds taken by Chandra X-ray Observatory, NASA and Harvard and Smithsonian Center for Astrophysics. The purple colored areas are hypothesized regions of dark matter, whose density increases with the luminosity of the purple color



Source: Constraints on physics of gas and dark matter from cluster mergers

Figure 2: The strong gravitational lensing features a distorted image of a farther blue galaxy from behind the yellowish fuzzier elliptical galaxy members of the cluster CL0024+17. All of the elliptical galaxies in the center are gravitationally bound and related, where there's no correlation between the distorted blue galaxy with them. The image of the blue galaxy is refracted into many tangential arcs, which the scale of the Einstein Ring is unreproducible with only the luminous mass of the galaxy cluster. Hence, proving that there's a large dark matter halo around the cluster. The cross point sourced light are nearby stars in our own galaxy (the star angle created by the shape of optical mirrors in the Hubble space telescope)



Source: NASA/ESA/M.J. Jee (John Hopkins University).

Gravitational lensing around galaxy clusters (see Fig. 2) cannot be produced with only the luminous mass deduced from the galaxy and also reveals the presence of a massive dark matter component that should be a factor of about 6 more massive than ordinary matter.

2. Rotational Velocity

Dark matter contributes to explaining the most relevant dynamical aspects of galaxies. In particular, the galactic rotation curves, such as for the Milky Way, have been widely used to estimate the dark matter density. The star velocities are expected to decrease with the square root of the radius for distances beyond the disk size if only visible, i.e. baryonic matter is present. In fact, the density of gas and stars decreases sharply beyond the Galactic disk. If we consider that only visible mass contributes to the velocity at radius R, which is given by:

$$V(R) = \sqrt{\frac{GM(R)}{R}}$$

Then the mass M(R) would be constant for R>galactic disc radius and thus the velocity would decrease with the square root of radius.

However, the measurements from Jeremiah Ostriker et al. in Princeton and Jaan Einasto et al [9] in Estonia indicates that the rotation curve data is approximately constant after reaching the end of the disk. This means that the stars at the rim of the galaxy are orbiting almost at the same speed as the stars within the outer bounds of the disk, despite being less luminous matter present. Hence, there must be invisible mass surrounding the galaxy to add the mass component and let the stars have a high orbital velocity. This additional invisible matter, called dark matter, should have a density profile $\propto r^{-2}$ in order to provide a velocity profile constant in radius.

3. Purpose

Following the research of dark matter density, I use the traditional method of evaluating rotational curves because it is a strong indicator of reflecting the dark matter density distribution in the galaxy, as proven by various historical research. In particular, I have selected GAIA DR2 data that is the currently newest measurement. Different papers have taken these data to extract the rotational velocity in the Milky Way. Most of them pointed out that there seems to be a decreasing shape of the velocity between 10 and 30 kpc. I decided to use the data released by Sofue 2025 [20] to get a reliable measurement of the rotational velocity of stars in the Milky Way. In particular, we consider data from 0.02 kpc to 95 kpc, which covers the bulge, disk and outer halo of the galaxy where dark matter should contribute the most. Based on Sofue's paper on the NFW fit with GAIA DR2 Data, I have elaborated on other mainstream models of Einasto, Isothermal, Burkert, Moore as well as NFW, to verify the accuracy and universality of the rotational curve shapes.

4. Data

The data we used is taken from [20], which takes into account the latest GAIA data to estimate the star rotational velocities. We have used this reference because it is among the newest and most updated releases of the rotational velocity data.

First, we have used a simplified method to estimate the dark matter density parameters. In particular, we have considered the values of the local dark matter density and total dark matter mass as reported in [7]. The local dark matter density is 0.3 GeV/cm³ while the total dark matter mass within 60 kpc is $4.7 \times 10^{11} M_{\odot}$(solar masses). We have first fixed the normalization using the value of the local dark matter density and then we have found the scale radius using the total dark matter mass. The constants we applied are reported in Table 1.

When using this method we find the values of ρ_s and r_s reported in the bottom part of Table 2.

By comparing these numbers with the ones of Ref [7] we note that the values we find are comparable to the one reported in that reference. Therefore, our results and the method applied seem reasonable. We now proceed in the next section with a more precise method which relies on the rotational velocity data.

Table 1: Physical constants and parameters used in the rotation curve and dark matter density modeling

Parameter	Value	Description
C_ρ	$2.63 \times 10^7\ M_\odot\ kpc^{-3}$ / (GeV cm^{-3})	Density conversion factor
R_0	8.178 kpc	Solar radius from Galactic center
ρ_0	0.36 GeV cm^{-3}	Local dark matter density
R_{max}	120.0 kpc	Maximum radius considered
M_{tot}	$4.7 \times 10^{11}\ M_\odot$	Total mass of the Milky Way
G	$4.30091 \times 10^{-6}\ km^2\ s^{-2}\ kpc / M_\odot$	Gravitational constant (astrophysical units)
$\alpha_{Einasto}$	0.11	Shape parameter (Einasto–Burkert hybrid modeling)

Table 2: Initial estimates for local dark matter scale density and scale radius across various DM profiles using approximation from Cirelli et al.

Parameter	NFW	Einasto	Isothermal	Moore	Burkert
R_s (kpc)	24.50	35.51	4.40	30.39	12.68
ρ_s (GeV/cm^3)	0.18	0.02	1.38	0.10	0.71

5. Methodology

We applied mathematical models from [20], and used a python program to fit the data of the rotational velocity applying the following models of dark matter density.

Navarro-Frenk-White (NFW) [16]: $\rho_{NFW}(r) = \rho_s \frac{r_s}{r}\left(1 + \frac{r}{r_s}\right)^{-2}$

Einasto [9]: $\rho_{Ein}(r) = \rho_s\ exp\ exp\ \left\{-\frac{2}{\alpha}\left[\left(\frac{r}{r_s}\right)^{\alpha} - 1\right]\right\}$

Isothermal [3]: $\rho_{Iso}(r) = \frac{\rho_s}{1+(r/r_s)^2}$

Burkert [5]: $\rho_{Bur}(r) = \frac{\rho_s}{(1+r/r_s)(1+(r/r_s)^2)}$

Moore [14]: $\rho_{Moo}(r) = \rho_s \left(\frac{r_s}{r}\right)^{1.16} \left(1 + \frac{r}{r_s}\right)^{-1.84}$

ρ_s represents a normalization parameter that acts as a scaling factor for the overall mass concentration. r represents the distance from the center of the galaxy or the center of the dark matter halo and it is taken from the table in the appendix, which is the independent variable. r_s is the typical scale radius of the dark matter density profile, that determines where the profile changes shape. For $r \ll r_s$, the density profile is relatively shallow ($\rho_s \propto r^{-1}$), while $r \gg r_s$, the density profile drops off much more steeply ($\rho_s \propto r^{-3}$).

For α used in the Einasto model, we have taken the value of 0.11, which is stated in [7]. It is also a shape parameter, which allows the Einasto profile to adjust how quickly the density transitions from the center to the outer edges. A smaller α results in a more divergent center.

The first density profile is NFW and it is a cuspy profile that increases as r approaches 0. NFW and Moore profiles arise from cold dark matter N-body simulations, where gravitational collapse of collisionless particles naturally leads to centrally concentrated "cuspy" density distributions. These profiles predict a steep increase in density toward the Galactic center due to hierarchical merging and violent relaxation processes. The NFW density actually diverges for r=0. This is cured typically by fixing a constant density for very small distances from the Galactic center.

The Einasto profile is also categorized as a cuspy profile which however is not divergent at r=0. It is more of an intermediate profile that describes how the logarithmic slope varies with radius smoothly. Its hybrid position has led to some excellent fits with both theoretical and observational data, including this paper. The Isothermal and Burkert are instead flat for small distances from the center and they are typically called cored profiles.

The density profiles for the NFW, Moore, Burkert, Isothermal and Moore models are almost identical beyond the core radius r_s, where they tend to $\propto r^{-3}$. The differences among the models appear for distances well within the Solar circle. The cuspy models (NFW and Moore models) predict a steep increase of density toward the center with a singularity at r=0. Typically this divergence is cured by introducing a very central

core. The cored halo models predict a mild and low density plateau in the center with the peak densities not much differing from each other within a factor of two. In contrast, the Burkert and isothermal profiles are phenomenological models introduced to better match observational data, especially in dwarf galaxies, where central density cores rather than cusps are observed. These "cored" profiles feature a nearly constant density in the inner region, avoiding the divergence present in cuspy models.

Most of the Dark Halo models predict lower density in the innermost galaxy by two to several orders of magnitudes than the bulge's density. This implies that the Dark Halo does not much influence the kinematics in the inner galaxy. Namely, it is practically impossible to detect the Dark Matter cusp by analyzing the Rotation Curves. Only the Moore model predicts cusp density exceeding the bulge's density in the very center at r < ~0.1 pc, whereas the applicability of the model to such a small sized region is not obvious.

We have taken the rotational velocity data from table 5 and 6 in [20].

As a physical model for the star, gas and dark matter we include De Vancouleurs Bulge, exponential disk, and dark halo, evaluating the velocity equation relative to radius as follows. ρ_s is the local dark matter density which is 0.36 GeV/cm³ [20].

The mass for each model is obtained via numerical integration, where r' is the component (bulge, disk, halo) distance with respect to the Galactic center.

$$M(r) = 4\pi \int_0^r \rho(r')\, r'^2\, dr'$$

5.1 De Vaucouleurs Bulge

The Milky Way is a SB III galaxy, therefore it contains a bar shaped bulge. We couldn't use simple models like the Hernquist bulge that assumes the bulge area to be homogenous. Therefore, we used the Vaucouleur's law because it provides a good first-order approximation to the radial mass distribution of the central bulge, which is justified because the azimuthally averaged stellar density in the bulge region follows a steep centrally concentrated profile similar to that observed in elliptical galaxies. Dark matter is not nearly as evident as in other parts of the galaxy, yet it still exerts an extent of influence in the Galactic dynamic.

This part correlates to the immediate steep rising limb of Fig. 2, 3, 4, 5 as enclosed mass increases rapidly coming out away from the real center of the Milky Way. The density of stars, gas and other objects is very high and they provide a huge boost to the velocity curve.

Below we report the key equations to find from the surface mass density, the density profile, the mass and the rotational velocity.

Surface mass density from the law: $\Sigma_b(R) = \Sigma_{be} exp\left[-7.6695\left(\left(\frac{R}{R_b}\right)^{1/4} - 1\right)\right]$ [10]

Volume Mass Density: $\rho(r) = \frac{1}{\pi}\int_r^\infty \frac{d\Sigma_b(x)}{dx}\frac{1}{\sqrt{x^2-r^2}}dx$

Mass inside radius R: $M(R) = 4\pi \int_0^R r^2\rho(r)dr$

Circular velocity for Bulge: $V_b(R) = \sqrt{\frac{GM(R)}{R}}$

We use the common De Vaucouleurs law Surface Mass Density profile to model the central bulge, where the surface mass density is postulated to be proportional to the empirical optical profile of surface brightness, where Σ_{be} is the value at radius R_b enclosing a half of the integrated surface mass. It is important to consider that the De Vaucouleurs surface profile, also the exponential disk, has a finite value at the center. The volume mass density ρ(r) at radius r for a spherical bulge is calculated using the second equation, and enclosed average mass is calculated using the third equation.

In principle, the corresponding three-dimensional density distribution of the surface projected density profile should be obtained through Abel deprojection. However, the exact deprojection does not yield a simple analytical expression and is computationally expensive to evaluate numerically.

Therefore, we adopt an analytic approximation to the deprojected profile of the form

$$Abel's\ deprojection: \rho_b(r) = \rho_{0,b} exp\left[-\left(\frac{r}{R_b}\right)^4\right], \quad where\ \rho_{0,b} = 5 \times 10^4 [6]$$

which captures the strongly concentrated nature of the bulge while remaining numerically stable and efficient for integration. This approximation reproduces the key physical behavior of the De Vaucouleurs profile, namely a steep central density and rapid decline with radius.

This approach allows us to compute the enclosed mass and rotational velocity without performing explicit Abel deprojection, while maintaining a physically reasonable description of the bulge.

5.2 Exponential Disk

The exponential disk model is widely supported by both observations and theory. Stellar disks in spiral galaxies, including the Milky Way, are observed to follow an exponential surface density profile as a natural consequence of angular momentum conservation during galaxy formation. Large surveys and photometric studies i.e. GAIA we've used in this paper confirms that the Milky Way's stellar disk can be well approximated by an exponential profile with a scale radius of a few kiloparsecs.

Though the disk and bulge models we've corroborated had excluded the galactic bar, spiral arms, and non-axisymmetric structures and other significant structures, they provide a robust and widely used approximation for large-scale mass distribution. This level of approximation is sufficient for modeling the rotation curve, where the dominant factor is the radial distribution of enclosed mass rather than local structural irregularities.

Surface Mass Density: $\Sigma_d(R) = \Sigma_{d0} exp\ (-R/R_d)$ [19]

Rotation Curve for a Thin Exponential Disk:

$V_d(R) = \sqrt{4\pi G \Sigma_d R_d x^2 [I_0(x)K_0(x) - I_1(x)K_1(x)]}$ [8]

Where $x = R/(2R_d)$

Total Disk Mass: $M_{disk} = 2\pi\Sigma_d R_d^2$

Where the surface density is the sum of the exponential of the radius we enclose to our distance to the center of the Milky Way Rd. The rotation curve is plotted with the Bessel Function via scipy.special with modules $I_0(x), K_0(x), I_1(x), K_1(x)$.

5.3 Dark Halo

Dark halo is where most of the mass is present as dark matter. Here, the effect of visible matter is negligible, hence we directly apply the theoretical NFW, Einasto, Moore, Isothermal and Burkert models to this region. After obtaining the dark matter density ρ_{DM} from the models. Its slower decrease in density than baryonic components corresponds to the level-off of velocity as radius increases. We use an integration that assumes the halo is perfectly spherical to integrate the enclosed mass. Note here we assume that dark matter doesn't interact or form non-uniform density clumps in the halo, or is an oblate spheroid due to the rotation and mass bent of the galaxy.

5.4 Combining the Velocities

The velocities for each component can be combined with this formula:

$$V(R) = \sqrt{\sum V_i^2} = \sqrt{R\frac{\partial \sum \Phi_i}{\partial R}}$$

Where it can be simplified to:

$$V(R) = \sqrt{V_{BH}(R)^2 + V_b(R)^2 + V_d(R)^2 + V_h(R)^2}$$

Where V_{BH} is the velocity derived from the mass of the central black hole Sagittarius A* in the galaxy, it could be largely neglected where R>0.1 kpc on the scale of the whole galaxy. Therefore, we can deduce that the final velocity is the vector sum of De Vancouleur's bulge $V_b(R)$, Exponential disk $V_d(R)$ and Dark Halo $V_h(R)$. By inverting the process, we would be able to deduce the mass of dark matter present in a specific area of the galaxy.

Figure 3: Rotation curve plotted when using the Burkert model.

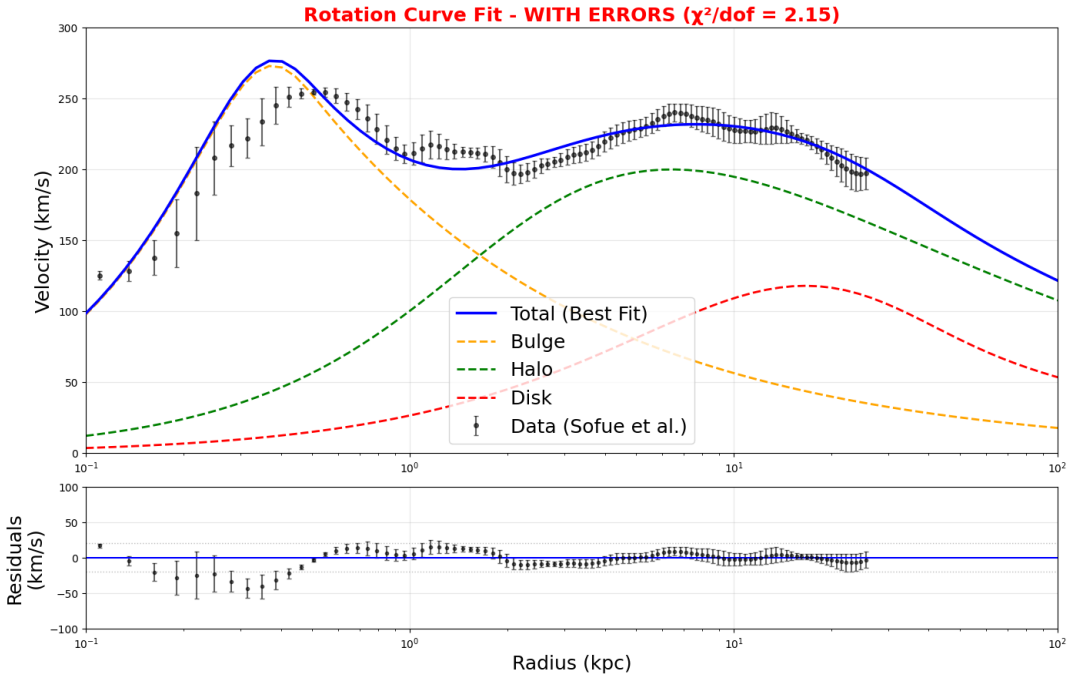


Figure 4: Rotation curve plotted found with the isothermal model

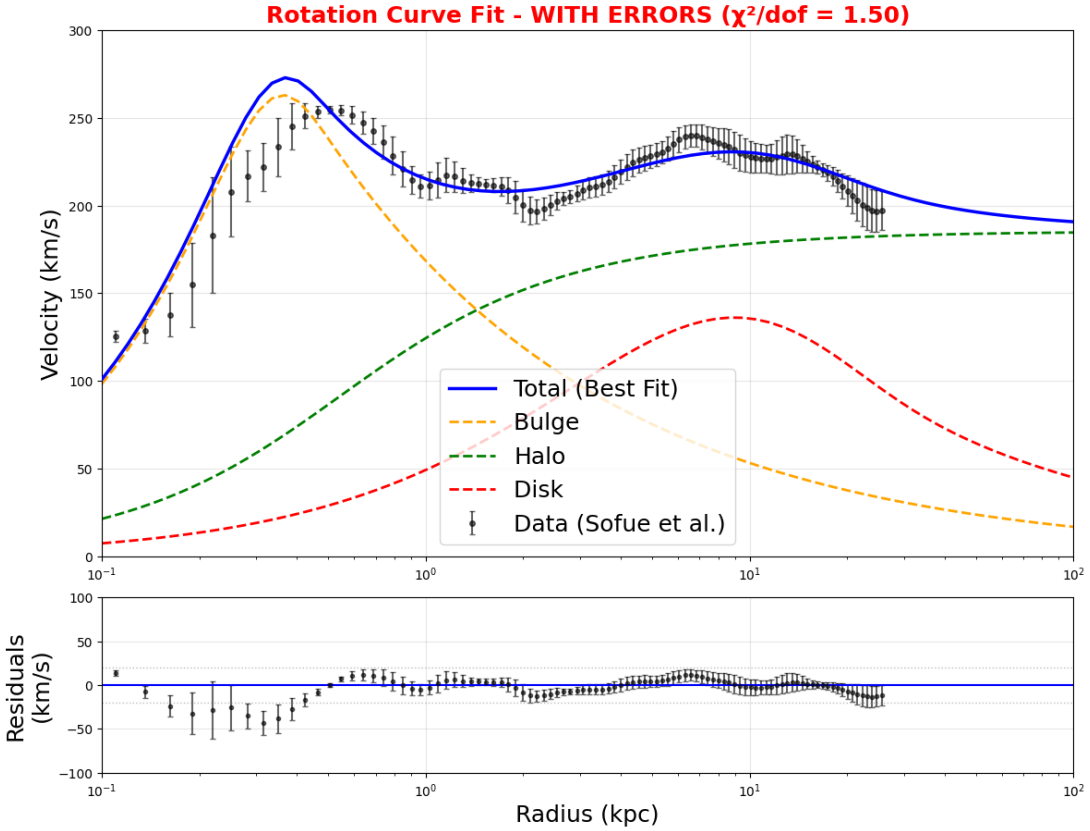


Figure 5: Rotation curve plotted by Moore model

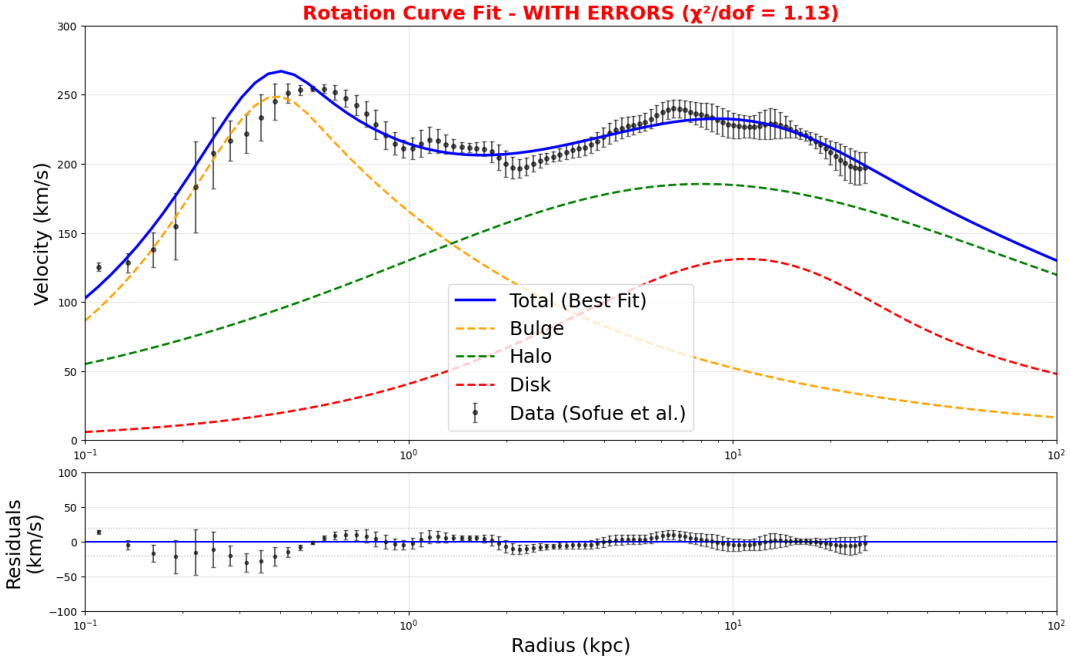


Figure 6: Rotation curve plotted by Einasto model. This is the model that provides the best fit with a chi-square value of 0.96

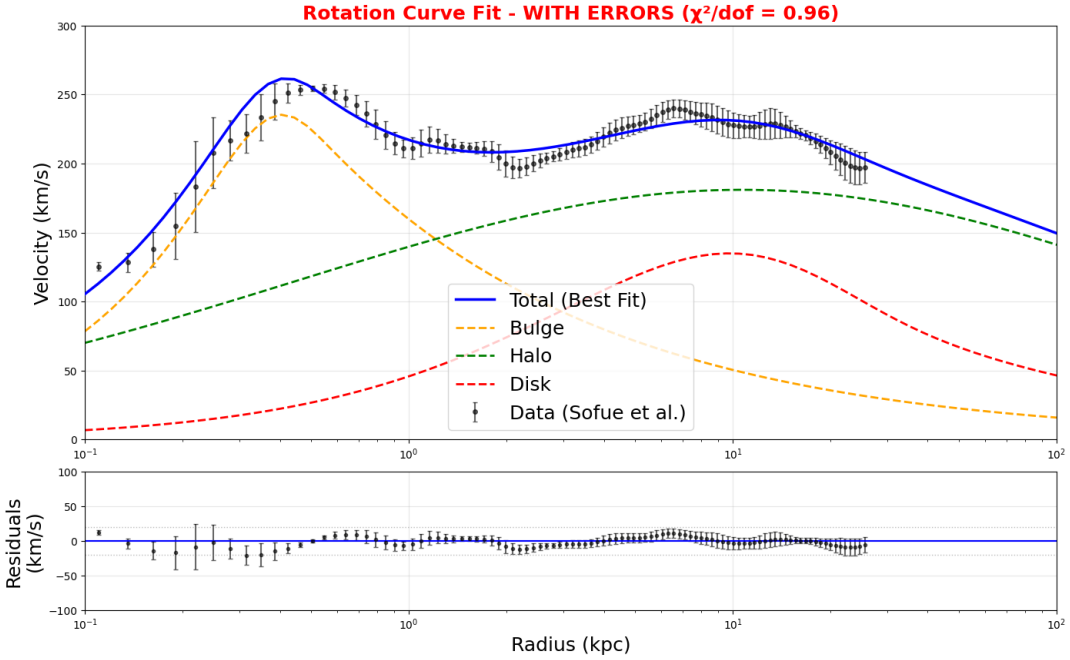
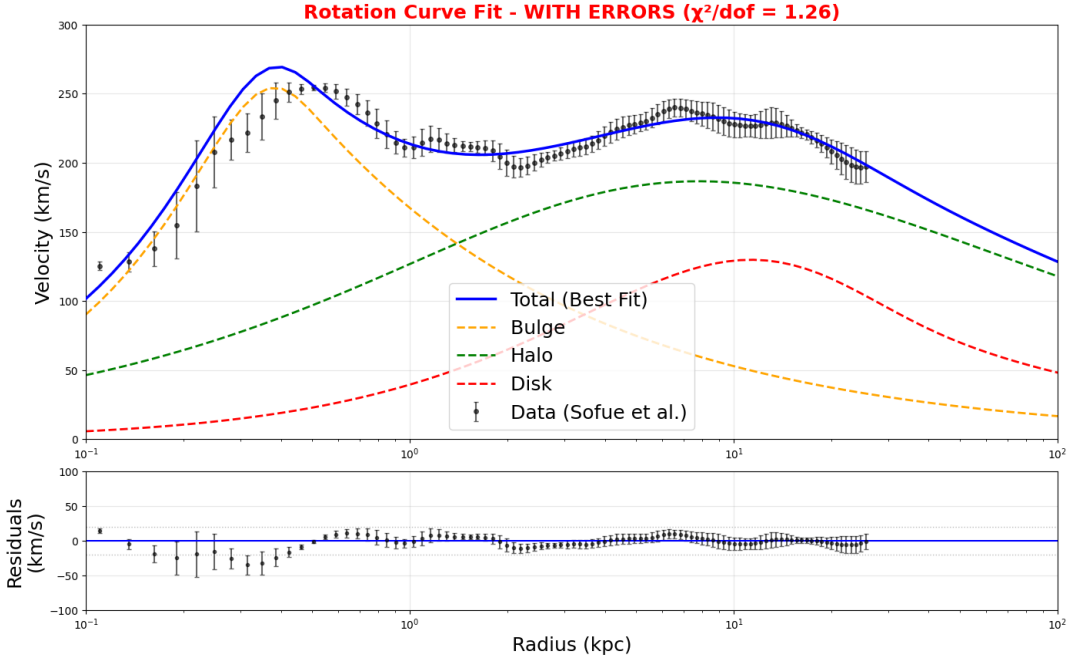


Table 3: Best-fit parameters for Galactic components across various Dark Matter profiles, including halo scale radius and density.

Parameter	NFW	Einasto	Isothermal	Moore	Burkert
$\log(\Sigma_b)$	10.66 ± 0.02	10.54 ± 0.03	10.73 ± 0.02	10.62 ± 0.03	10.73 ± 0.02
R_b (kpc)	0.33 ± 0.01	0.36 ± 0.01	0.32 ± 0.01	0.34 ± 0.01	0.33 ± 0.01
$\Sigma_d(R)$ ($M_\odot$/kpc^2)	8.49 ± 0.05	8.58 ± 0.04	8.63 ± 0.03	8.51 ± 0.05	8.24 ± 0.05
R_d (kpc)	5.27 ± 0.38	4.55 ± 0.27	4.18 ± 0.19	5.12 ± 0.36	7.75 ± 0.86
R_s (kpc)	3.60 ± 0.18	4.62 ± 0.48	0.49 ± 0.06	4.47 ± 0.25	1.98 ± 0.04

Figure 7: Rotation curve plotted according to NFW model



6. Results

We obtain the best fit values for the model parameters by running the iminuit minimization package. Instead in order to plot the best-fit model compared with the data we use matplotlib. In the minimization procedure, we used chi square statistics to evaluate the consistency of parameters through the different 5 models:

$$\chi^2 = \sum_i \frac{\left(V_{obs,i} - V_{model,i}\right)^2}{\sigma_i^2}$$

With initial parameters $\log(\Sigma_b)$=10.5, R_B= 0.4 kpc, $\Sigma_d(R)=9M_\odot$/kpc², R_d=3 kpc, R_s=1 kpc

Figure 3, 4, 5, 6, 7 reports the data of the rotational velocity together with our best-fit theoretical curves. We report the contribution of each component together with the total one.

For each graph, the red dotted line represents the rotation velocity curve of the disk. The yellow dotted line represents the rotation velocity curve of De Vancouleur's bulge. The green dotted line represents the rotation velocity curve of the dark halo applied with that specific model. R_s and ρ_s are the parameters we produced when we fitted the total dark matter enclosed mass radius and local dark matter density when using the method with Cirelli et al [7].

To conclude from our graphs from the five mainstream dark matter models, our major residuals difference is located in the primary peak of near 0.9 kpc from the Galactic center that in any case has its largest experimental errors. Einasto has proven to be the smallest deviating, i.e. best, model with only 0.96 chi square while Burkert has the largest on 2.15. Since Sofue's curve was only evaluated using the NFW model, we expect some minor deviants on the other models. Hence, it is truly a surprise that our plotted Einasto was actually more fitting than the NFW used in both cases. We postulate that it is due to the Einasto model being a less cusp model, which more fittingly with the result to avoid infinity approximation at the galactic center, as the NFW model does. We would further evaluate on the best fit parameters to avoid iminuit program going into a fake local minima when fitting the curve.

The previous evaluation coincides with the expected outcome. In general, the steep increase within 1 kpc is due to the bulge concentrate at that distance, where the surge of around 0.3 kpc occurs at every curve is an indicator of a baryonic dense possible bar within the bulge. The contributions of the bulge have the steepest increase and decrease occurring within 0.25 kpc averagely for each of the model graphs, predicting that the baryonic matter concentration reaches a local maximum around the same radius. Intermediately, the disk plays

a crucial role within 20 kpc, where the rotation curve seems to have a less steep falling limb where the velocity decreases from around 240 km/s at the peak to around 210 km/s at the local minimum around 1.45 kpc. This also encloses off the solar radius of 8.178 kpc, indicating that our solar system's motion is primarily subjective of the disk, with contributions from the outer halo but too distant to be affected by the bulge. The contributions of the disk shown in red dashed line has the lowest baseline of a few km/s and the farthest peak occurring at 10.1 kpc. This may be explained with the outer boundaries of the Milky Way's disk is also around 10 kpc wide and baryonic matter density slowly decreases going farther away from the outskirts of the disk into the halo. The smoother and more flattened shape of the disk component could be explained as the baryonic matter concentration isn't as dense as the bulge, so the increase in velocity doesn't drop drastically like as in the boundary of bulge and disk, instead diffuses slowly out. The halo contribution peaks before the disk, have a higher baseline about 50 km/s and the most flattened shape out of all three component velocities. The flat shape is due to the consideration that dark matter surrounds the galaxy in a homogeneous sphere uniformly, where its contribution to different radius is generally equal. The earlier peak is likely due to model assumptions and fitting, where we would like to evaluate more in detail since the halo expectedly should play a more outstanding role after the disk has passed.

The velocities of mass would increase rapidly coming to around 5 kpc, where because more mass (both dark matter and visible matter) are enclosed in the region, we would expect an increase to velocity as it is proportional to mass. The curve reaches a peak at 18 kpc, where the disk of the galaxy approximately ends. Here most visible matter is enclosed and we would expect the rotational curve to decrease exponentially onwards if only considering normal matter, as there is less visible matter lying outside of the galaxy's disk into the halo, so there isn't enough mass to support the objects going at high velocities. However, the rotational curve seems to flatten out beyond 10 kpc, proving the likeability of existence of dark matter as there must be extra invisible mass contributing the objects at such far distances outside of the main disk to orbit at higher speeds. The rotational curve slowly decreases as dark matter diffuses out to form a halo and most mass is already enclosed, hence less mass lies beyond 60 kpc to sufficiently withstand the objects moving at higher speeds.

When the simpler method from [7] is used, which features just calibrating on total dark matter mass and local dark matter density, we find very different average values on dark matter parameters of the dark matter halo radius R_c 21.50±12.78 kpc and local dark matter density ρ_s0.48±0.57 GeV/cm³. In summary, if we use Rotation Curves, the values are more precise and physically motivated.

Table 4: Statistical Summary of Galactic Parameters and Model Goodness-of-Fit (χ2). Parameters derived via the rotational curve plot velocity method

Parameter (Average ± SD)	Value
$\log(\Sigma_b)$	10.66 ± 0.08
R_b (kpc)	0.34 ± 0.02
$\Sigma_d(R)$ ($M_\odot/kpc^2$)	8.49 ± 0.15
R_d (kpc)	5.37 ± 1.40
R_s (kpc)	3.03 ± 1.77
Model Profile	χ^2 Value
Einasto	0.96
Isothermal	1.13
NFW	1.26
Moore	1.50
Burkert	2.15

From Table 4, we have obtained the logarithm of Σ_b for the normalization factor of the bulge to be averaged at 10.7 according to de Vancouleur's model. R_b The bulge radius is taken to be around 0.34 kiloparsecs. The normalization of the disk factor has some variance of lowest 8.24 in the Burkert model, highest 8.63 in the isothermal model. This variation is likely due to the differences in considering factors of the models, and some limits on the Burkert model that we have tried to minimize. For the exponential disk radius, the values range from 4.18 to 7.75, which was also affected by the Burkert modelling with its value of 7.75 being an outlier.

We tried to narrow the chi square down to smaller than 2, but 2.15 is the smallest given. Finally, for the radius of the dark matter halo, NFW, Einasto, Moore seems to agree with the range from 3.60-4.47, while

Burkert obtains 1.98kpc and surprisingly Isothermal a questionable 0.49kpc, despite having a chi square of 1.50. In conclusion, the models unify for logarithmic bulge normalization factor and radius of the bulge. Farther from the center of the galaxy, discrepancies began to appear and increased to the radius of dark matter halo, which has a range of 0.49 to 4.62 kpc.

The residuals graph mainly showed greater deviation for all models where R<0.7kpc. This is due to there being more celestial bodies and interstellar mediums that will have complex multi-body gravitational interactions with each other, thus influencing the plot of stellar velocities. We also assumed an axisymmetrical disk and circular orbits that neglected non-circular motions, bar dynamics and vertical structure that would play a crucial role in influencing the orbits of stars and mapping stellar velocities in real life. Once past 1 kpc, the residuals graph was fitted almost linearly with Sofue's values. This shows as entering the less baryonic matter dense regions, our postulations on dark matter influences on stellar velocities do coalesce with Sofue's research. It is also worth mentioning that the reference curve from [20] was only fitted with NFW profile, which would provide some explanations for the inconsistency at certain levels (e.g. at peaks) with certain models following a different philosophy. On the other hand, this highlights that it is truly a surprise that the same NFW model used didn't produce the best but the Einasto model did. The preference for the Einasto profile suggests that the Milky Way halo may have a smoother inner density transition than predicted by pure NFW simulations. We would follow up on this matter to delve deeper into the reasons.

7. Summary

In sum, we have used rotational curve data (from stellar rotational velocity), and evaluated the formula of velocity for the different Galactic components with respect to radius. We evaluated and tested first on Cirelli et al. 's simplified method to find the typical radius of dark matter halo and the local dark matter density using as input and beacon the total dark matter mass and local dark matter density.

Then we have applied a more refined method which relies on deriving the dark matter density profile by fitting the rotation curve data.

We combined velocities with the vector sum of De Vaucouleur's bulge with Abel's deprojection grid fit, exponential disk, and dark matter halo models components, to evaluate best fit parameters for each dark matter model with iminuit and plot stellar velocity rotation curves. However, the De Vaucouleurs bulge, exponential disk and the previous dark matter models all assume that gas and other celestial objects orbit the center of the galaxy in circles, neglecting the dynamic flow of the central bar, stellar streams, spiral arms, expanding rings and other asymmetrical or symmetrical structures located inside the galaxy. This hinders the accuracy of the results from the model, and needs to be combined and rectified with more observational data. We hope our findings would be a humble stepping stone to the research of dark matter, galaxy structure and evolution. It would raise great hopes within us if our writing has invoked a perspective in the evolution of the galaxy's dynamics.

The results of the Rotation Curve graphs are all located in the 0.5-2.5 chi square range, which has some limitations while generally accurate. We would spend further evaluations of the Burkert and other models, trying to optimize the fit and fine tune the best fit parameters. We would update our radius data with newer GAIA DR3 or even DR4 data releasing later this year, keeping the RC up to date and evaluate for further research.

References

[1] Baba, J. (2025). Bar-driven Streaming Motions Mimic a Massive Bulge in the Inner Milky Way. [online] arXiv.org. Available at: https://arxiv.org/abs/2507.12702 [Accessed 13 Oct. 2025].

[2] Balazs, C., Torsten Bringmann, Kahlhoefer, F. and White, M. (2024). A Primer on Dark Matter. Alphaxiv.org. [online] doi:https://doi.org/10.1103/RevModPhys.90.045002.%201605.04909.

[3] Begeman, K.G., Broeils, A.H. and Sanders, R.H. (1991). Extended Rotation Curves of Spiral galaxies: Dark Haloes and Modified Dynamics. Monthly Notices of the Royal Astronomical Society, 249(3), pp.523–537. doi:https://doi.org/10.1093/mnras/249.3.523.

[4] Beordo, W., Crosta, M. and Lattanzi, M.G. (2024). Exploring Milky Way rotation curves with Gaia DR3: a comparison between ΛCDM, MOND, and General Relativistic approaches. [online] arXiv.org. Available at: https://arxiv.org/abs/2407.12482 [Accessed 13 Oct. 2025].

[5] Burkert, A. (1994). The Structure of Dark Matter Halos in Dwarf Galaxies. The Astrophysical Journal, 447(1). doi:https://doi.org/10.1086/309560.

[6] Ciotti, L. (1999). Inversion of the Abel Equation for Toroidal Density Distributions. [online] arXiv.org. Available at: https://arxiv.org/abs/astro-ph/9903056 [Accessed 31 Mar. 2026].

[7] Cirelli, M., Corcella, G., Hektor, A., Hütsi, G., Kadastik, M., Panci, P., Raidal, M., Sala, F. and Strumia, A. (2011). PPPC 4 DM ID: a poor particle physicist cookbook for dark matter indirect detection. Journal of Cosmology and Astroparticle Physics, 2011(03), pp.051–051. doi:https://doi.org/10.1088/1475-7516/2011/03/051.

[8] Dehnen, W. and Binney, J. (1998). Mass models of the Milky Way. Monthly Notices of the Royal Astronomical Society, [online] 294(3), pp.429–438. doi:https://doi.org/10.1111/j.1365-8711.1998.01282.x.

[9] Einasto, J. and Einasto, M. (1999). Dark Matter in Groups and Clusters of Galaxies. [online] ar5iv. Available at: https://ar5iv.labs.arxiv.org/html/astro-ph/9909437 [Accessed 31 Mar. 2026].

[10] G. de Vaucouleurs (1958). Photoelectric Photometry of the Andromeda Nebula in the UBV System. The Astrophysical Journal, 128(465), pp.465–465. doi:https://doi.org/10.1086/146564.

[11] Kapteyn, J.C. (1922). First Attempt at a Theory of the Arrangement and Motion of the Sidereal System. The Astrophysical Journal, 55, p.302. doi:https://doi.org/10.1086/142670.

[12] Laurin Söding, Bartel, R.L. and Philipp Mertsch (2025). Local dark matter density from Gaia DR3 K-dwarfs using Gaussian processes. Monthly Notices of the Royal Astronomical Society, [online] 542(4), pp.2987–2997. doi:https://doi.org/10.1093/mnras/staf1391.

[13] Massey, R., Kitching, T. and Richard, J. (2010). The dark matter of gravitational lensing The dark matter of gravitational lensing 2. [online] Available at: https://arxiv.org/pdf/1001.1739 [Accessed 2 Feb. 2026].

[14] Moore, B. (1994). Evidence against dissipation-less Dark Matter from Observations of Galaxy Haloes. Nature, [online] 370(6491), pp.629–631. doi:https://doi.org/10.1038/370629a0.

[15] NASA (2006). Bullet Cluster. [online] Available at: https://chandra.harvard.edu/graphics/resources/handouts/lithos/bullet_lithos.pdf.

[16] Navarro, J.F. (1996). The Structure of Cold Dark Matter Halos. Symposium - International Astronomical Union, [online] 171(9508025), pp.255–258. doi:https://doi.org/10.1017/s0074180900232452.

[17] Navarro, J.F., Ludlow, A., Springel, V., Wang, J., Vogelsberger, M., White, S.D.M., Jenkins, A., Frenk, C.S. and Helmi, A. (2009). The diversity and similarity of simulated cold dark matter haloes. Monthly Notices of the Royal Astronomical Society, 402(1), pp.21–34. doi:https://doi.org/10.1111/j.1365-2966.2009.15878.x.

[18] Navarro, J.F. and White, S. (1993). Simulations of dissipative galaxy formation in hierarchically clustering universes - I: Tests of the code. Monthly Notices of the Royal Astronomical Society, [online] 265(2), pp.271–300. doi:https://doi.org/10.1093/mnras/265.2.271.

[19] Sofue, Y. (2020). Rotation Curve of the Milky Way and the Dark Matter Density. [online] arXiv.org. Available at: https://arxiv.org/abs/2004.11688 [Accessed 13 Oct. 2025].

[20] Sofue, Y. and Kohno, M. (2025). The inner rotation curve of the Milky Way. [online] arXiv.org. Available at: https://arxiv.org/abs/2509.23581 [Accessed 13 Oct. 2025].

[21] Woudenberg, H.C. and Helmi, A. (2024). First measurement of the triaxiality of the inner dark matter halo of the Milky Way. Astronomy & Astrophysics, [online] 691(A&A Volume 691, November 2024 A277), p.A277. doi:https://doi.org/10.1051/0004-6361/202451743.

Funding

This research received no external funding.

Data Availability

The obtained rotation curve is listed in the tables in the appendix. The survey data used in this article are available electronically, as described in the text in the reference section.

Conflicts of Interest

The authors declare no conflict of interest.

Acknowledgment

We would like to thank the extensive work and guidance provided by Dr. Mattia DiMauro, who has been there to help during the whole research process. He has provided countless insights and been a driving force to lift the research out of troubles. The “PPPC 4 DM ID: A Poor Particle Physicist Cookbook for Dark Matter Indirect Detection” [Cirelli.M, Corcella.G et al] has served as a fundamental structure and guide leading us to this new field. It has proved to be especially practical in providing the background knowledge and supplemental details of the field. The continuous research conducted by Dr.Sofue has been proved insightful for the thesis in the further research on dark matter density distribution. His Figure 2 graph has served as a reference and the data in the appendix table 5 and 6 are the fundamental nutrient input of this paper.

Open Access

This chapter is licensed under the terms of the Creative Commons Attribution-NonCommercial 4.0 International License (http://creativecommons.org/licenses/by-nc/4.0/), which permits any noncommercial use, sharing, adaptation, distribution and reproduction in any medium or format, as long as you give appropriate credit to the original author(s) and the source, provide a link to the Creative Commons license and indicate if changes were made.

The images or other third party material in this chapter are included in the chapter's Creative Commons license, unless indicated otherwise in a credit line to the material. If material is not included in the chapter's Creative Commons license and your intended use is not permitted by statutory regulation or exceeds the permitted use, you will need to obtain permission directly from the copyright holder.

